Research Journal of Chemical Sciences ISSN 2231-606X
Vol. **4(9),** 88-100, September **(2014)** *Res. J. Chem. Sci.*

Nano iron oxide loaded Poly (Acrylonitrile-co-Acrylic acid) hydrogel applied as Novel adsorbent for Effective removal of Toxic Cd^{2+} ions using Fixed-bed Micro column technology

Neeraj Sharma and Alka Tiwari*
Department of Chemistry, Govt. V.Y.T. PG. Autonomous College Durg- 491001, CG, INDIA

Available online at: www.isca.in, www.isca.me
Received 12th January 2014, revised 1st May 2014, accepted 12th September 2014

Abstract

This study applies super paramagnetic nano iron oxide particles loaded poly (Acrylonitrile-co-acrylic acid) hydrogel as adsorbent for the removal of toxic cadmium ions from aqueous solution using column adsorption. Experiments were carried out as a function of liquid flow rate (1 – 3 ml min^{-1}), initial feed of Cd (II) concentration (0.25 – 1 mg dm^{-3}) and bed depth (0.25 – 1 cm). The results showed that a flow rate of 1 ml min^{-1}, inlet Cd (II) concentration of 1 mg dm^{-3} and a bed depth of 1 cm were most feasible. The total adsorbed quantities, equilibrium uptakes and total removal percents of Cd (II) related to the effluent volumes were determined by evaluating the breakthrough curves obtained at different flow rates, inlet Cd (II) concentration and bed depth respectively. The bed depth service time (BDST), Thomas, Yoon-Nelson, Bohart-Adams and Wolborska kinetic models were used to analyze the experimental data and the model parameters were evaluated. The experimental data correlated well with calculated data using Yoon-Nelson equation.

Keywords: Super paramagnetic nano iron oxide**,** Hydrogel**,** column adsorption**,** breakthrough curves**,** kinetic modeling.

Introduction

Large quantities of heavy metals are released into the natural environment by many natural and human activities which generate a number of environmental problems[1]. Cadmium is considered to be the most toxic heavy metal ion which reaches in our natural water resources as a result of various industrial activities like mining, ceramics, metal plating, metallurgical alloying, phosphate fertilizers, pigments, batteries, etc[2-4]. It is non-biodegradable and tends to accumulate in living organisms, causing the significant threats to both public health and environment[5]. Cadmium poisoning even in low dosages is responsible for causing renal disorder, bone fraction, high blood pressure, kidney damage, and destruction of red blood cells[6]. Cadmium ions influence the enzyme activity if zinc ions are replaced by them in some metalo-enzymes[7]. WHO described the permissible limit for Cd (II) is 0.01 mg dm^{-3}.

In order to remove heavy metals from polluted water, a number of methods namely chemical precipitation, filtration, ion exchange, electrochemical treatment, oxidation or reduction, reverse osmosis and adsorption have been developed[5,8-10]. The expensive cost, low efficiency, labor-intensive operation, and lack of selectivity in the treating process are some of the major disadvantages found in the above methods[11]. To minimize the environmental pollution caused by heavy metal ions, "adsorption" is one of the most promising techniques as compared to various conventional methods. The major advantages of adsorption technique are low cost, regeneration of the adsorbent, high efficiency of metal ions removal and the possibility of metal recovery.

In the present work, we explore the novel sorbent "super paramagnetic nano iron oxide loaded poly (Acrylonitrile-co-acrylic acid) hydrogel" (nano iron oxide loaded PANA hydrogel) which shows high affinity for Cd (II) ions. The efficient removal of cadmium ions by the sorbent was studied as function of different flow rate, bed depth and inlet Cd (II) concentration in a fixed-bed column system. This study has applied empirical models by Thomas, Yoon-Nelson, Adams-Bohart and Wolborska for describing cadmium removal from aqueous solution on a fixed-bed of nano iron oxide loaded PANA hydrogel. Nano particles of iron-oxide with high surface energy and surface area have strong adsorption capability, high magnetic properties and involve easy and rapid separation of adsorbent from solution with respect to many inorganic ions and organic matters. The combined technique of sorption and magnetic separation holds the advantageous flexibility, ecofriendly characteristic and recovery of heavy metals is very important and inspiring. Super paramagnetic iron oxide nano particles [mostly magnetite (Fe_3O_4) or maghemite (γ-Fe_2O_3)] with tailored surface chemistry have been widely used experimentally for numerous applications which require nano particles having high magnetization values and sizes smaller than 100 nm with overall narrow particle size distribution[12].

Material and Methods

Material: The monomers acrylonitrile and acrylic acid were purchased from Loba Chemi, Mumbai and Himedia, Mumbai, India respectively. N, N'-methylene-bis-acrylamide (cross-linker), potassium per sulphate (initiator), anhydrous ferric

chloride and ferrous chloride tetra hydrate were purchased from Molychem, Mumbai, India. Deionized water was used throughout the experiments.

Synthesis of nano iron oxide loaded PANA hydrogel: To a mixture of acrylonitrile and acrylic acid (1:1 ratio) the cross linker (N, N'-methylene-bis-acrylamide) and initiator (potassium per sulphate) were added and heated at 70^{o}C in an electric oven for 1 h. The copolymeric hydrogel so formed was washed with distilled water and cut into small uniform pieces. For in-situ magnetization, these pieces were equilibrated in an aqueous solution of ferrous chloride and ferric chloride for 24 h. The Fe^{3+}/Fe^{2+} loaded pieces of copolymer were then dipped in conc. ammonia solution and kept overnight. The Magnetic hydrogel was then washed thoroughly with distilled water, dried and crushed into a fine powder.

TEM analysis: The average particle size, size distribution and morphology of iron oxide nano particles were examined by TEM analysis (TECNAI – G20 TEM at a voltage of 200 kV). The solvent dispersion of the particles was drop – cast onto a carbon coated copper grid and the grid was air dried at ambient conditions (25 ± 1^{0}C) before loading into the microscope.

AFM analysis: The morphology and diameter of magnetite nano particles was examined by contact mode AFM (NS-E, Digital Instrument INC, USA) using silicon nitrate tip. The sample was prepared for AFM analysis by placing a few drops of the suspension of Fe_3O_4 in 50% HCl on a cleaved mica sheet (UGC-DAE, Indore, India).

FTIR analysis: FTIR spectra of bare and Cd^{2+} ions loaded adsorbent were recorded using Varian Vertex FTIR Spectrometer. (UGC-DAE, Indore, India).

XRD analysis: The crystalline nature of the magnetic nano particles loaded PANA hydrogel was studied on a Bruker D8 advanced X-ray Diffractometer with scanning range of 20^{o}-80^{o} (2θ) using Cu Kα radiation with wavelength of 1.5406Å. (UGC-DAE, Indore, India).

Preparation of stock solution: Stock solution of Cd (II) of 1000 mg dm^{-3} was prepared by dissolving 0.179g $CdCl_2$ (AR) in 100 ml deionized water. Suitable concentrations of Cd (II) for column experiments were prepared by diluting the stock solution with deionized water.

Analytical techniques: The concentration of Cd (II) ions was determined using Atomic Absorption Spectrometer (Varian AA-24-OFS model).Each experiment was carried out in triplicate under identical conditions to get the mean values.

Fixed-bed adsorption micro column study: Fixed-bed adsorption experiments were performed in a column made of polyethylene having an inner diameter of 0.5 cm and a height of 10 cm, at a constant temperature of 25^{0}C. The column was packed with different bed heights of nano iron oxide loaded PANA hydrogel on a glass-wool support (figure-1). The experiments were performed at pH 4. The batch experimental results showed that the adsorption rate was high at pH 4. A known concentration of cadmium solution was allowed to pass through the bed at a constant flow rate (1 ml min^{-1}) in a down-flow manner. The cadmium solution was then collected at different time intervals until the column reached exhaustion and the concentration of Cd (II) ions was determined by Atomic Absorption Spectrometer. The important design parameters such as column bed height, flow rate of metal solution into column and initial concentration of metal solution have been investigated.

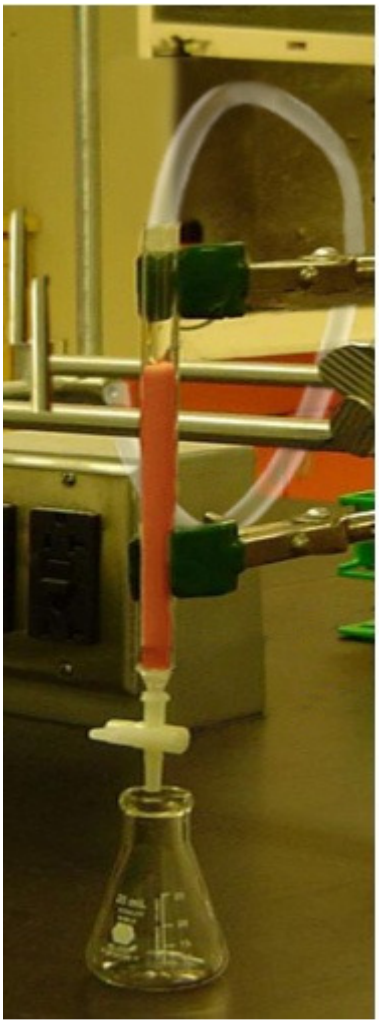

Figure-1
Photograph showing the experimental set up for fixed-bed column study

Analysis of column data: The efficiency of the column was evaluated by determining breakthrough curves. To examine the dynamic nature and operation of a adsorption column, breakthrough time and shape of breakthrough curve are the main parameters. The adsorptive nature of Cd (II) ions in a

fixed-bed column is shown by breakthrough curves and is expressed as adsorbed metal ion concentration (C_{ad}), which may be defined as the ratio of outlet metal ion concentration to inlet metal ion concentration as a function of volume of outlet or time for a given bed depth. The breakthrough volumes V_B and exhaustion volumes V_E are the effluent volume at breakthrough time (t_b) and exhaustion time (t_e), respectively. Effluent volume (V_{eff}) can be calculated from equation (1):

$$V_{eff} = Qt_{total} \quad (1)$$

Where t_{total} and Q are the total flow time (min) and volumetric flow rate (ml min^{-1}). The area under the breakthrough curve (A) obtained by integrating the adsorbed concentration (C_{ad}; mg dm^{-3}) versus t (min) plot can be used to find the total adsorbed metal quantity (maximum column capacity). Total adsorbed metal quantity (q_{total}; mg) in the column for a given feed concentration and flow rate (Q) is calculated from equation (2):

$$q_{total} = \frac{Q \cdot (C_0 - C_t) \cdot t_{total}}{1000} \quad (2)$$

Total amount of metal ion sent to column (m_{total}) is calculated from equation (3):

$$m_{total} = \frac{C_0 \cdot Q \cdot t_{total}}{1000} \quad (3)$$

Total removal percent of Cd (II) is the ratio of the maximum capacity of the column (q_{total}) to the total amount of Cd (II) sent to column (m_{total}) from equation (4):

$$\text{Total removal (\%)} = \frac{q_{total}}{m_{total}} \times 100 \quad (4)$$

Equilibrium metal uptake (q_{eq}) (or maximum capacity of the column) in the column is defined by equation (5) as the total amount of metal sorbed (q_{total}) per g of sorbent (X) at the end of the total flow time:

$$q_{eq} = \frac{q_{total}}{X} \quad (5)$$

Modeling of column dynamics: The sorption performance of the Cd (II) through the column was analyzed by BDST, Thomas, Yoon-Nelson, Adams-Bohart, Wolborska models starting at concentration ratio, C_t/C_0 = breakthrough point until $C_t/C_0 > 0.90$ that is 90% breakthrough for cadmium by considering the safe water quality standards and operating limits of mass transfer zone of a column.

Bed depth – service time model (BDST): BDST is a simple model, which states that bed depth (Z) and service time (t) of a column bears a linear relationship. Equation (6) shows the linearized form of the model.

$$t = \frac{N_0 Z}{C_0 Q} - \frac{1}{K_a C_0} \ln\left(\frac{C_0}{C_t} - 1\right) \quad (6)$$

Where C_t is the breakthrough metal ion concentration (mg dm^{-3}), N_0 the sorption capacity of bed (mg/L), Q the flow rate (ml min^{-1}) and K_a is the rate constant (L/mg.min).

Thomas model: The Thomas model is one of the most general and widely used. The model is applicable in system with a constant flow rate and no axial dispersion, and its behavior matches the Langmuir isotherm and the second-order reversible reaction kinetics. The linearized form of the model is given by equation (7).

$$\ln\left(\frac{C_0}{C_t} - 1\right) = \frac{K_{Th} q_0 M}{Q} - \frac{K_{Th} C_0}{Q} V \quad (7)$$

In this equation k_{Th} (ml/mg min) is the Thomas rate constant, q_0 (mg/g) is the equilibrium adsorbate uptake, Q (ml min^{-1}) is the flow rate and V (ml) is effluent volume. C_t is the concentration of metal ion at time t and C_0 is the initial metal ion concentration.

Yoon-Nelson model: To inspect the breakthrough nature of Cd (II) ions on nano iron oxide loaded PANA hydrogel, a theoretical model was tested which was developed by Yoon-Nelson. This model is based on the assumption that the rate or decrease in the probability of adsorption for each adsorbate molecule is proportional to the probability of adsorbate adsorption and the probability of adsorbate breakthrough on the adsorbent. The Yoon-Nelson model not only is less complicated than other models but also requires no detailed data concerning the characteristics of adsorbate, the type of adsorbent and the physical properties of adsorption bed. The linearized model for a single component system is expressed by equation (8).

$$\ln\left(\frac{C_t}{C_0 - C_t}\right) = K_{YN} t - \tau \cdot K_{YN} \quad (8)$$

Where k_{YN} (min^{-1}) is the Yoon-Nelson rate constant and τ is the time required for 50% adsorbate breakthrough (min) and t is the sampling time (min). C_t is the concentration of metal ion at time t and C_0 is the initial metal ion concentration.

For a given bed:

$$q_{0YN} = \frac{C_0 \cdot Q \cdot \tau}{1000\, X} \quad (9)$$

Where, q_{0YN} is adsorption capacity, C_0 is initial metal ion concentration, Q is the flow rate, X is the weight of adsorbent and τ is the 50% breakthrough time.

Adams- Bohart model: This model was established based on the surface reaction theory and it assumed that equilibrium is not instantaneous. Therefore the rate of adsorption was proportional to both the residual capacity of the adsorbent and the concentration of the sorbing species. The mathematical equation of the model can be written as:

$$\ln\left(\frac{C_t}{C_0}\right) = K_{AB} \cdot C_0 \cdot t - K_{AB} \cdot q_{AB} \cdot \frac{Z}{Q} \quad (10)$$

Where C_0 and C_t are the inlet and outlet adsorbate concentrations (mg dm^{-3}), respectively, K_{AB} is rate constant (L/mg min), q_{BA} is removal capacity (mg/L), Z (cm) is the bed depth, Q is linear flow velocity (ml min^{-1}) and t is service time (min).

Value of removal capacity q in mg/g is calculated as follows:

$$q = \frac{q_{AB} \cdot BV_s}{m} \quad (11)$$

Where q is removal capacity (mg/g), BVs is fixed bed volume (L) and m is mass of the bed (g).

Wolborska model: The next simplified adsorption model was derived by Wolborska. The linearized form of the model is given by equation (12).

$$\ln\left(\frac{C_t}{C_0}\right) = \frac{\beta_a \cdot C_0}{q} \cdot t - \frac{\beta_a \cdot Z}{Q} \quad (12)$$

Where C_0 and C_t are the inlet and outlet adsorbate concentrations (mg dm^{-3}), respectively, β_a is rate constant (min^{-1}), q is removal capacity (mg/g), Z (cm) is the bed depth, Q is linear flow velocity (ml min^{-1}) and t is service time (min).

Column desorption study: To carry out column desorption study, 0.1 M HNO_3 solution was added at a flow rate of 1 ml min^{-1} at room temperature taking 1 cm bed depth for 240 min and then washed thoroughly with hot distilled water and then could be reused for further adsorption experiments.

Results and Discussion

TEM analysis: The shape, size and morphology of iron oxide nano particles were determined through TEM imaging. The TEM images of nano particles show almost cubic iron oxide particles with an average size of less than 10 nm, as shown in figure-2. Size of these nano particles lie within the range 1-9 nm. It should be noted, however, that the majority of the particles were scattered, a few of them showing aggregates indicate stabilization of the nano particles. The results represented by TEM images concluded that the particle size of individual nano particles seem to be 1-10 nm, whereas majority of nano particles exhibit smaller sizes i.e. 5 and 8 nm.

AFM analysis: The morphology of the magnetite nano particles, using contact mode AFM, was found to be spherical, having size distribution in two different diameter (height) ranges of 10-20 nm (mean height: 15 nm) and 40-110 nm (mean height: 50 nm and 80 nm) as shown in figure-3. However, some larger particle size in figure may be a result of agglomeration of smaller magnetite nano particles in order to reduce the inherent large surface energies for magnetite nano particles.

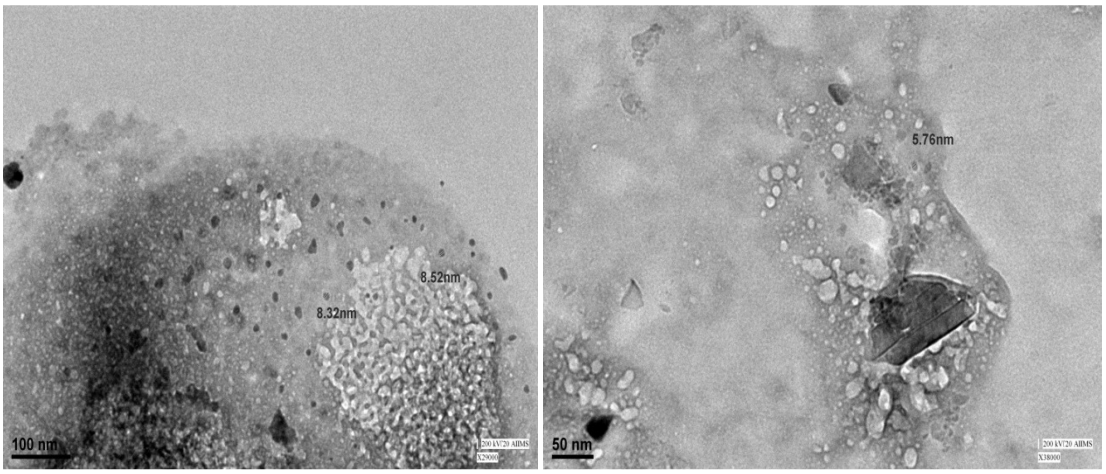

Figure-2
Transmission Electron Micrograph of iron oxide nano particles

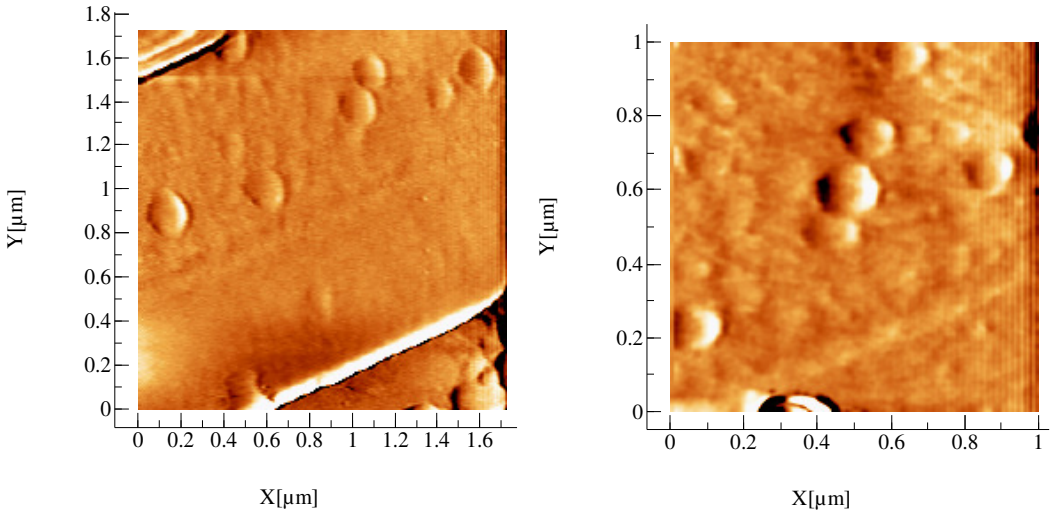

Figure-3
AFM topographic images of magnetic nano particles on mica

FTIR analysis: Fourier Transform Infrared Spectroscopy (FTIR) of bare and Cd^{2+} adsorbed nano iron oxide loaded PANA hydrogel are shown in figure 4 (a) and (b) respectively. The adsorption band at 530 cm^{-1} is due to C-C≡N. The 1075 cm^{-1} band is assigned to the CH vibration mode. The absorption band at 1250 cm^{-1} is due to the bending mode of the methane (-CH) group coupled with the rocking mode of the methylene ($-CH_2$) group. The bands appear at 1220-1270, 1345-1375 and 1465 cm^{-1} are assigned to C-H vibration modes.

In the FTIR spectra of the copolymer, the absorption bands at 1000-1300 cm^{-1} might be due to C-O stretching vibration, the strong band at 1730 cm^{-1} is due to the carboxyl (C═O) stretching vibration of the acrylic acid. The strong band at 2240 cm^{-1} is assigned to nitrile (C≡N) group. The band at 2850-2960 cm^{-1} is due to stretching vibration of CH_2 and the absorption bands at 3500-3560 cm^{-1} are assigned to stretching vibration of –OH. The characteristic peak at 566.69 cm^{-1} relates to Fe-O group, which indicates the loading of nano iron oxide particles on PANA hydrogel because the surface of iron-oxide with negative charges has an affinity towards PANA hydrogel, the magnetite nano particles could be loaded into protonated copolymer by the electrostatic interaction and chemical reaction through N,N'-methylene-bis-acrylamide cross linking. The FTIR analysis indicated the band due to N, N'-methylene bis acrylamide at 3358 cm^{-1},1660 cm^{-1}, 1604 cm^{-1} and 1407 cm^{-1} attributed to N-H stretching, C=O stretching, N-H bending and C-N stretching respectively, which are the characteristics of the amide ($CONH_2$) group. In figure-4 (b) a slight change in shape and intensity of absorbance (due to -C≡N, $-CONH_2$ and –COOH groups) has been noticed which indicates that electron rich nitrogen of acrylonitrile and amide group of N, N'-methylene-bis-acrylamide moiety and $-COO^-$ group of acrylic acid moiety involve in removal of Cd^{2+} ions. Change in the peak position and intensity for Fe-O group stretching from 566.69 to 551 cm^{-1} indicates that Cd^{2+} ions coordinate with electron rich oxygen of magnetite nano particles (Fe_3O_4).

XRD analysis: The XRD pattern for the nano iron oxide loaded PANA hydrogel is shown in figure-5. Five characteristic peaks (2θ = 30.09, 35.44, 43.07, 56.96 and 62.55), marked by their indices [(511), (311), (400), (511) and (440)], were observed for super paramagnetic PANA hydrogel. The position and relative intensities of all diffraction peaks in the figure 5 match well with those from the JCPDS file No. 89-5984 for magnetite (Fe_3O_4) and reveal that the prominent phase formed is Fe_3O_4 and the resultant nano particles of super paramagnetic iron oxide were pure magnetic with cubic structure. Magnetite is obtained according to the reaction:

$$2FeCl_3 + FeCl_2 + 8NH_4OH \rightarrow Fe_3O_4 + 8NH_4Cl + 4H_2O$$

Mechanism of uptake: A probable mechanism for Cd^{2+} ions uptake by nano iron oxide loaded PANA hydrogel can be explained as shown below: i. Carboxylate groups ($-COO^-$) of acrylic acid moiety of copolymer interact with Cd^{2+}. ii. Cd^{2+} ions co-ordinate with the electron rich nitrogen of nitrile group of acrylonitrile moiety of copolymer. iii. In addition within the copolymer matrix, these Cd^{2+} ions may also co-ordinate with the electron rich oxygen of magnetite nano particles.

Column studies of adsorption of Cd (II) ions onto nano iron oxide loaded PANA hydrogel: Several operational factors such as bed depth (Z), flow rate (Q) and initial adsorbate concentration (C_0) affect the shape of a breakthrough curve and maximum capacity of the column. In this study, the effect of these parameters on breakthrough curve and maximum capacity of the column was investigated.

Effect of bed depth: Accumulation of metals in the fixed bed column is largely dependent on the quantity of sorbent added in the column[13]. The sorption breakthrough curves were obtained

by varying bed depth ranging from 0.25 to 1 cm at 1 ml min^{-1} flow rate and 3 mg dm^{-3} initial cadmium ion concentration, shown in figure-6. It was observed that breakthrough and exhaustion time increases with increasing bed depth due to the availability of more binding sites for adsorption of cadmium ions. With the increase in bed height, adsorption was found to be increased because of the increase in adsorbent quantity which resulted in increased adsorption sites. The values are given in table-1.

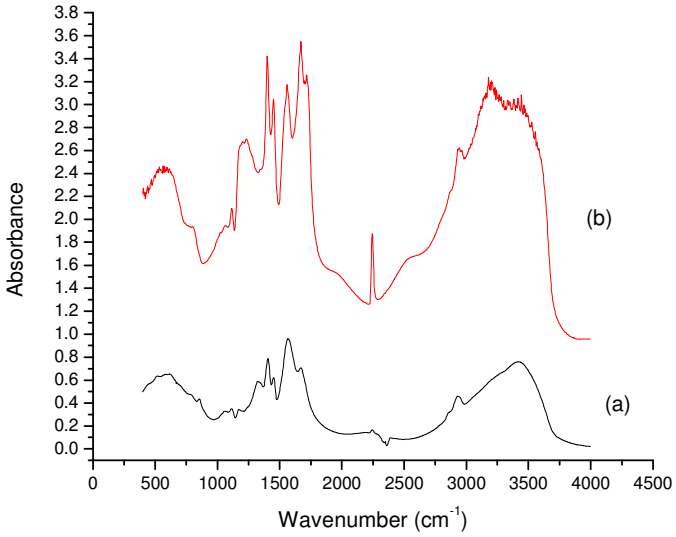

Figure-4
FTIR pattern of (a) nano iron oxide loaded PANA hydrogel before sorption of Cd (II) ions. (b) nano magnetite loaded PANA hydrogel after sorption of Cd (II) ions

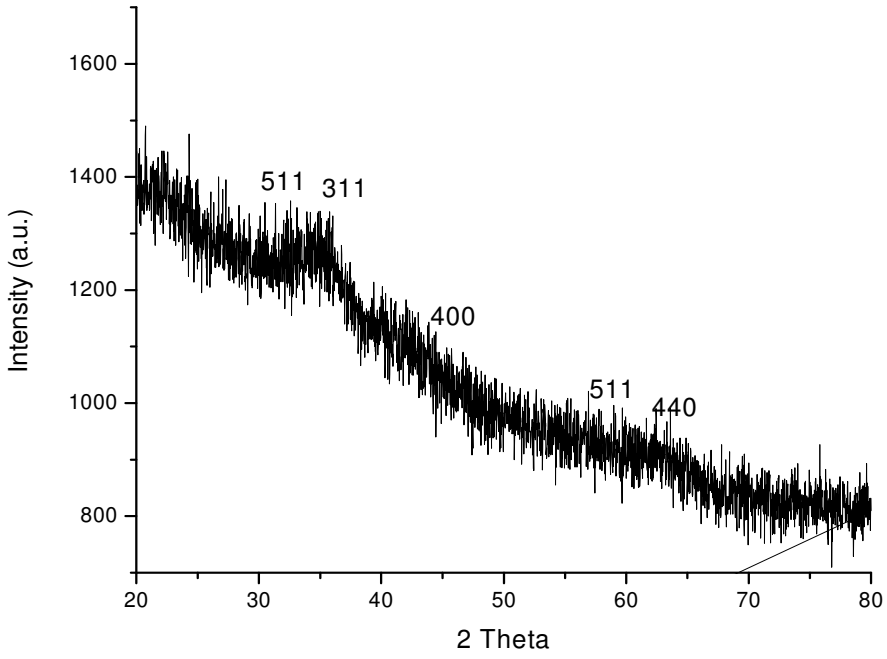

Figure-5
XRD pattern of nano iron oxide loaded PANA hydrogel

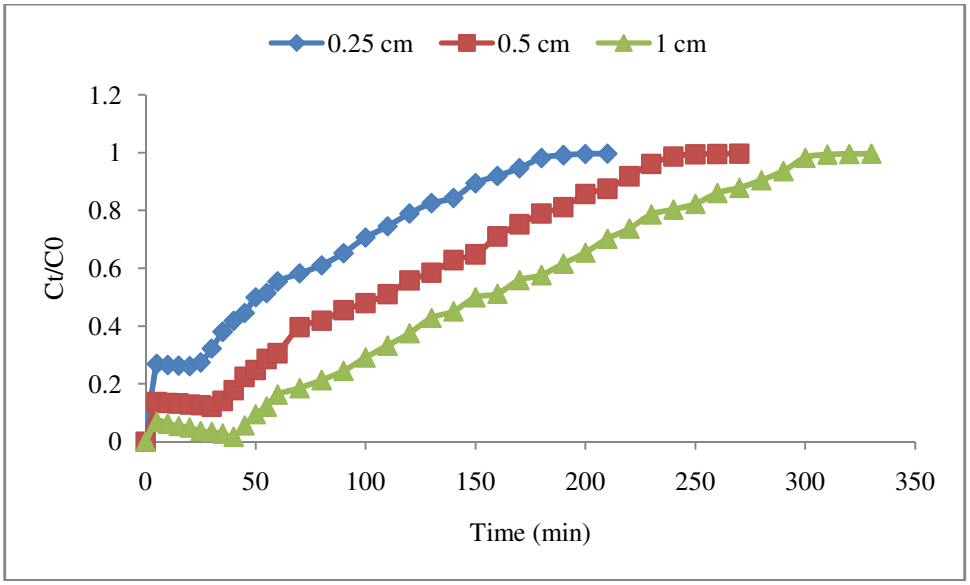

Figure-6
The effect of bed depth on breakthrough curve at temperature = 25 ± 0.2^{0}C, pH = 4, bed depth of nano iron oxide loaded PANA hydrogel = 0.25, 0.5 and 1 cm, flow rate = 1 ml min^{-1} and Cd (II) initial concentration = 3 mg dm^{-1}

Table- 1
The effect of bed depth on breakthrough curve at temperature = 25 ± 0.2^{0}C, pH = 4, bed depth of nano iron oxide loaded PANA hydrogel = 0.25, 0.5 and 1 cm and flow rate = 1 ml min^{-1} and Cd (II) initial concentration = 3 mg dm^{-3}

Bed depth (cm)	Flow rate (ml min^{-1})	Inlet cadmium ion concentration (mg dm^{-3})	t_{total} (min)	m_{total} (mg)	q_{total} (mg)	q_{eq} (mg/g)	Removal (%)
0.25	1	3	210	0.630	0.466	4.660	73.97
0.5	1	3	270	0.810	0.712	3.560	87.90
1	1	3	330	0.990	0.973	2.433	98.28

Effect of flow rate: The figure-7 shows effect of variation in feed flow rate on the adsorption of Cd (II) ions on nano iron oxide loaded PANA hydrogel which was investigated by varying the feed flow rate (1, 2 and 3 ml min^{-1}) at a constant adsorbent bed height of 1 cm and inlet adsorbate concentration of 3 mg dm^{-3}. It was observed that at higher flow rate, the front of the adsorption zone quickly reached the top of the column and resulted an early saturation of column. At lower flow rate a longer contact time, as well as a shallow adsorption zone was noticed. At higher flow rates a comparatively steeper curve with relatively breakthrough and exhaustion time was observed which resulted in less adsorption uptake[14].

Effect of initial cadmium ion concentrations: The effect of inlet cadmium concentration on the column performance was studied by varying the inlet concentration of cadmium between 1, 2 and 3 mg dm^{-3}, taking the same adsorbent bed depth (1 cm) and flow rate (1 ml min^{-1}). The figure-8 illustrated breakthrough curves, which show that the columns exhausted faster at higher adsorbate inlet concentration (3 mg dm^{-3}), hence gave a steeper curve showing an earlier breakthrough point. With the increase in adsorbate inlet concentration the breakthrough time (t_b) was found to decrease because of quick saturation of the column. An extended breakthrough curve was obtained by the decrease in inlet concentration, suggesting a higher volume of solution to be treated. This may be explained by the fact that a lower concentration gradient may cause a slower transport which will result in diffusion coefficient or mass transfer coefficient[15].

Column Kinetic study: The design and optimization of a fixed-bed sorption column need to employ some mathematical models, which must be used to describe and predict the experimental breakthrough curves, for possible scale up of process. The experimental adsorption data from the micro column studies was analyzed using BDST, Thomas, Yoon and Nelson and Adams-Bohart models to analyze the column performance.

BDST model: The BDST model which is the plot of service time against bed depth at a flow rate of 1 ml min^{-1} was linear (R^2 = 0.964), thus indicating the validity of this model for the present system (shown in figure-9). The rate constant (K_a) and sorption capacity of bed (N_0) were calculated from the intercept and slope of BDST plot respectively. The values of K_a and N_0

are given in table 4. The rate constant K_a characterizes the rate of solute transfer from the fluid phase to the solid phase. If the value of K_a is high, then even a short bed will avoid breakthrough, but with low K_a value, a progressively longer bed will be required to avoid breakthrough[16]. The performance of the bed may be predicted by using the parameter bed capacity (N_0). The residence time of the adsorbate solution increased inside the column with the increase in bed depth, which may permit the adsorbate molecules to be diffused deeper inside the adsorbent. Thus, by changing the service time, bed capacity will also be changed[17].

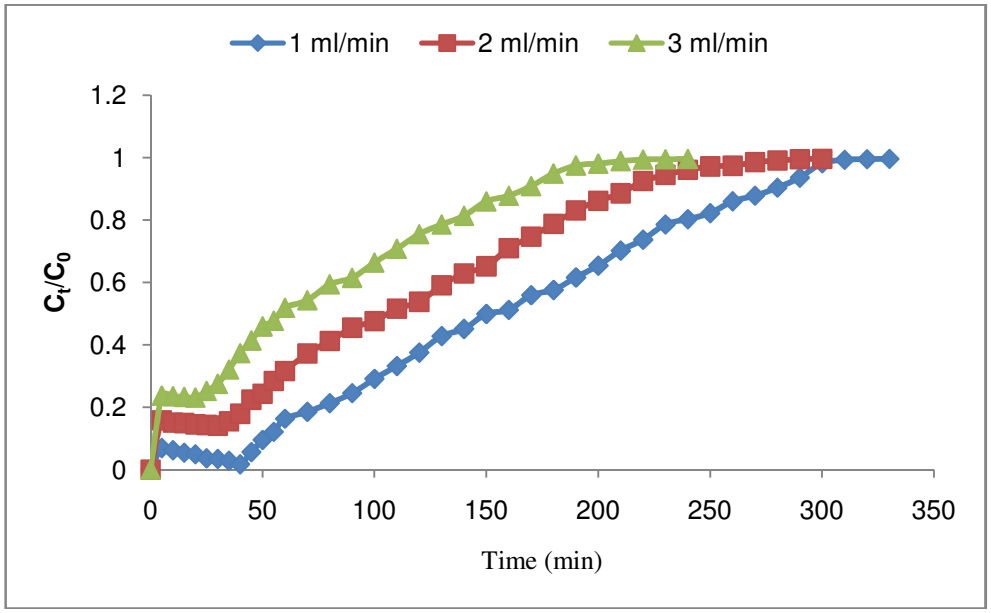

Figure-7

The effect of flow rate on breakthrough curve at Temperature = 25 ± 0.2^{0}C, pH = 4, flow rate = 1, 2 and 3 ml min^{-1}, bed height = 1 cm and Cd (II) initial concentration = 3 mg dm^{-3}

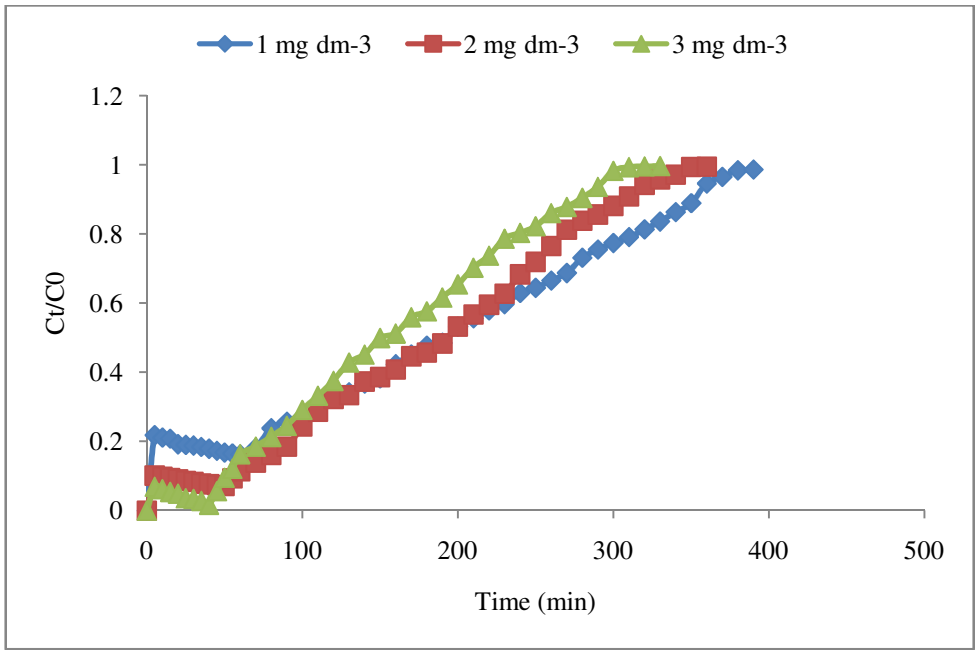

Figure-8

The effect of inlet adsorbate concentration on breakthrough curve at temperature = 25 ± 0.2^{0}C, pH = 4, initial Cd (II) ion concentration = 1, 2 and 3 mg dm^{-3}, bed depth = 1 cm and flow rate = 1 ml min^{-1}

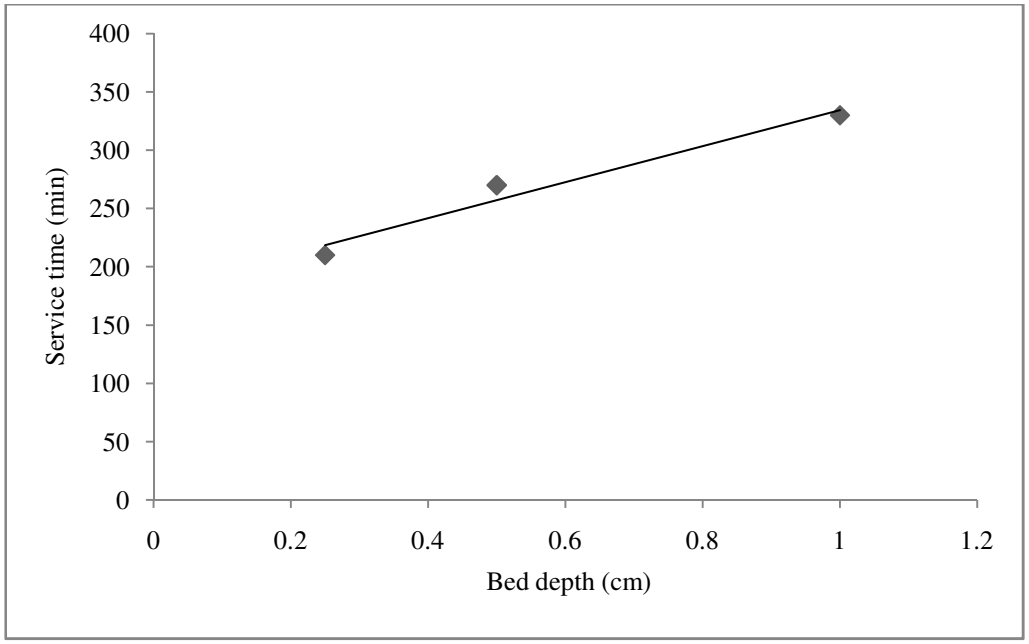

Figure-9
BDST model of Cd (II) ions adsorption by nano iron oxide loaded PANA hydrogel at temperature = 25 ± 0.2^{0}C, pH = 4, flow rate = 1ml min^{-1}, Cd (II) initial concentration = 3 mg dm^{-3}

Table-2
Results of breakthrough curve at different flow rates for adsorption of Cd (II) ions onto nano iron oxide loaded PANA hydrogel at temperature = 25 ± 0.2^{0}C, pH = 4

Flow rate (ml min^{-1})	Bed depth (cm)	Inlet cadmium ion concentration (mg dm^{-3})	t_{total} (min)	m_{total} (mg)	q_{total} (mg)	q_{eq} (mg/g)	Removal (%)
1	1	3	330	0.990	0.973	2.433	98.28
2	1	3	300	1.800	1.547	3.868	85.94
3	1	3	240	2.160	1.660	4.150	76.85

Table-3
Results of breakthrough curve at different inlet adsorbate concentration for adsorption of Cd (II) ions onto nano iron oxide loaded PANA hydrogel at temperature = 25 ± 0.2^{0}C, pH = 4

Inlet cadmium ion concentration (mg dm^{-3})	Bed depth (cm)	Flow rate (ml min^{-1})	t_{total} (min)	m_{total} (mg)	q_{total} (mg)	q_{eq} (mg/g)	Removal (%)
1	1	1	390	0.390	0.327	0.818	83.85
2	1	1	360	0.720	0.669	1.673	92.92
3	1	1	330	0.990	0.973	2.433	98.28

Table-4
Calculated constant of bed depth service time equation for adsorption of Cd (II) ions onto nano iron oxide loaded PANA hydrogel

Adsorbent	N_0 (mg/L)	K_a (L/mg/min)	R^2
nano iron oxide loaded PANA hydrogel	462.6	0.0075	0.964

Thomas model: The experimental data were applied with Thomas model to examine maximum capacity of sorption (q_0) and rate constant (K_{Th}). The K_{Th} and q_0 values were calculated from slope and intercept of linear plots of ln $[C_0/C_t) - 1]$ against t at different flow rates, bed heights and initial metal ion concentration using values from the column experiments (Figures are not shown). It can be concluded on the basis of the regression coefficient (R^2) and other parameters that the experimental data fitted well with Thomas model. The model parameters are listed in table 5. It was observed that by increasing concentration value of K_{Th} decreased while q_0 value showed a reveres trend. The maximum bed capacity (q_0) decreased with increase in flow rate as well as bed depth. K_{Th} values increased with increase in the flow rate but decreased with increase in bed depth. Similar trend has also been reported by Baral et al for Cr (VI) sorption by activated weed fixed bed column[18]. The Thomas model correlates well with the experimental data showing that the internal and external diffusion is not the rate limiting step[19].

Yoon-Nelson model: The values of K_{YN} and τ were evaluated from slope and intercepts of the linear graph between ln $[C_t / (C_0 - C_t)]$ versus t at different bed depths, flow rates and initial metal ion concentration (Figures are not shown). Values of K_{YN} and q_0 were found to increase with increase in flow rate and initial metal ion concentration and decrease with increase in bed depth. .With increase in initial metal ion concentration and flow rate, τ values decreased but increased with increase in bed depth. The values of K_{YN}, q_0 and τ are listed in table-6.

Adams- Bohart model: Linear plots of ln (C_t/C_0) against time, t at different bed depths, initial metal ion concentrations and flow rates were plotted (Figures are not shown). Values of K_{AB} and q_{AB} were calculated from the slope and intercept of the linear curves respectively and listed in table 7. Values of K_{AB} increased with increase in bed depth but decreased with increase in flow rate and initial metal ion concentration. This showed that the overall system kinetics was dominated by external mass transfer[20, 21]. However, q_{AB} values decreased for increasing bed depth but increased for increasing flow rate and initial metal ion concentration. Although, Adams-Bohart models gives a comprehensive and simple approach to evaluate column dynamics, its validity is limited to the range of condition used. Thus poor correlation coefficient reflects less applicability of this model[21].

Wolborska model: From the linear dependence of ln (C_t/C_0) versus t, the model parameters (i.e. β_a and q) can be determined. The linear dependence of the Adams-Bohart equation is the same and corresponds to the same mechanism as the Wolborska equation; therefore the same plots are used in calculation of parameters for both models. The maximum adsorption capacity, q and rate constant β_a increased with increase in initial cadmium ion concentration and flow rate but decreased with increase in bed depth.

Table-5
Thomas model parameters of adsorption of Cd (II) ions onto nano iron oxide loaded PANA hydrogel at different conditions using linear regression analysis

S.No.	Factors	Thomas Model Parameters		
		k_T (ml/min/mg)	q_0 (mg/g)	R^2
1.	Bed height (cm)			
(a)	0.25	7.3	1.766	0.985
(b)	0.5	6.3	1.665	0.980
(c)	1	6	1.206	0.979
2.	Flow rate (ml min^{-1})			
(a)	1	6	1.206	0.979
(b)	2	12.7	0.836	0.984
(c)	3	21	0.501	0.986
3.	Initial Cd (II) concentration (mg dm^{-3})			
	1			
(a)	2	11	0.493	0.993
(b)	3	8	0.914	0.985
(c)		6	1.206	0.979

Table-6
Yoon-Nelson model parameters of adsorption of Cd (II) ions onto nano iron oxide loaded PANA hydrogel at different conditions using linear regression analysis

S.No.	Factors	Yoon & Nelson Model Parameters			
		K_{YN} (min^{-1})	τ (min)	q_0 (mg/g)	R^2
1.	Bed height (cm)				
(a)	0.25	0.022	58.59	1.758	0.985
(b)	0.5	0.019	110.37	1.656	0.980
(c)	1	0.018	160.78	1.206	0.978
2.	Flow rate (ml min^{-1})				
(a)	1	0.018	160.78	1.206	0.978
(b)	2	0.019	111.84	1.678	0.984
(c)	3	0.021	66.81	1.503	0.986
3.	Initial Cd (II) concentration (mg dm^{-3})				
(a)	1	0.011	197.00	0.493	0.993
(b)	2	0.016	182.75	0.914	0.985
(c)	3	0.018	160.78	1.206	0.978

Table-7
Adams-Bohart model parameters of adsorption of Cd (II) ions onto nano iron oxide loaded PANA hydrogel at different conditions using linear regression analysis

S.No.	Factors		Bohart-Adams Model Parameters		
		K_{AB} (L/mg.min)	q_{AB} (mg/L)	q (mg/g)	R^2
1.	Bed height (cm)		2.075	4.358	0.899
(a)	0.25	2.3	1.304	1.760	0.889
(b)	0.5	2.7	0.796	0.657	0.862
(c)	1	3			
2.	Flow rate (ml min^{-1})				
(a)	1	3	0.796	0.657	0.862
(b)	2	2.7	1.301	0.976	0.907
(c)	3	2.7	1.436	0.862	0.892
3.	Initial Cd (II) concentration (mg dm^{-3})				
(a)	1	5	0.350	0.341	0.955
(b)	2	4	0.583	0.525	0.924
(c)	3.	3	0.796	0.657	0.862

Table-8
Wolborska model parameters of adsorption of Cd (II) ions onto nano iron oxide loaded PANA hydrogel at different conditions using linear regression analysis

S.No.	Factors	Wolborska Model Parameters		
		β_a (min^{-1})	q (mg/g)	R^2
1.	Bed height (cm)			
(a)	0.25	4.77	2.045	0.899
(b)	0.5	3.52	1.318	0.889
(c)	1	2.39	0.796	0.862
2.	Flow rate (ml min^{-1})			
(a)	1	2.39	0.796	0.862
(b)	2	3.51	1.318	0.907
(c)	3	3.88	1.454	0.892
3.	Initial Cd (II) concentration (mg dm^{-3})			
(a)	1	1.75	0.350	0.955
(b)	2	2.33	0.583	0.924
(c)	3	2.39	0.796	0.862

Desorption studies: Desorption results indicated 99.89% recovery of Cd (II) ions from the surface of the sorbent using 0.1 M HNO_3 in 5 hrs at 25°C temperature, the results are shown in figure-10. The nano iron oxide loaded PANA hydrogel showed almost the same metal ion adsorption capacity after the repeated regeneration. It may be stated that, in acidic medium, protons compete with Cd (II) ions and displace the maximum amount of adsorbed cadmium. Hence, ion exchange mechanism is important in connection with adsorption-desorption process for adsorbent.

Conclusion

The adsorbent "nano iron oxide loaded PANA hydrogel" has been found to be an effective, efficient and inexpensive adsorbent for Cd (II) removal from aqueous solution. The effects of bed depth, inlet feed concentration and flow rate on Cd (II) ion adsorption were investigated and the experimental breakthrough curves were obtained. The experiments were performed at 1 ml min^{-1} flow rate, 1 cm bed depth and 3 mg dm^{-3} inlet cadmium ion concentration at pH 4. It was observed that equilibrium metal uptake (q_0) increased with increase in flow rate and inlet cadmium ion concentration and decreased with increase in bed depth. Both breakthrough point and exhaustion time increased with increase in bed depth and inlet cadmium ion concentration and decreased with increase in flow rate. Thomas, Yoon and Nelson, Adams-Bohart and Wolborska kinetic models were used to describe the column adsorption kinetics. The experimental breakthrough curve was compared satisfactorily with the breakthrough profile calculated by Thomas and Yoon & Nelson method. The calculated column parameters could be scaled up for the design of fixed-bed columns for effective and efficient removal of toxic metal ions from water.

Acknowledgements

The authors would like to express thanks to the Department of Atomic Energy, BRNS-BARC, Mumbai, INDIA for providing financial assistance. Authors are also grateful to UGC-DAE Consortium for Scientific Research, Indore for FTIR and AFM analysis and AIIMS, New Delhi, India for TEM analysis.

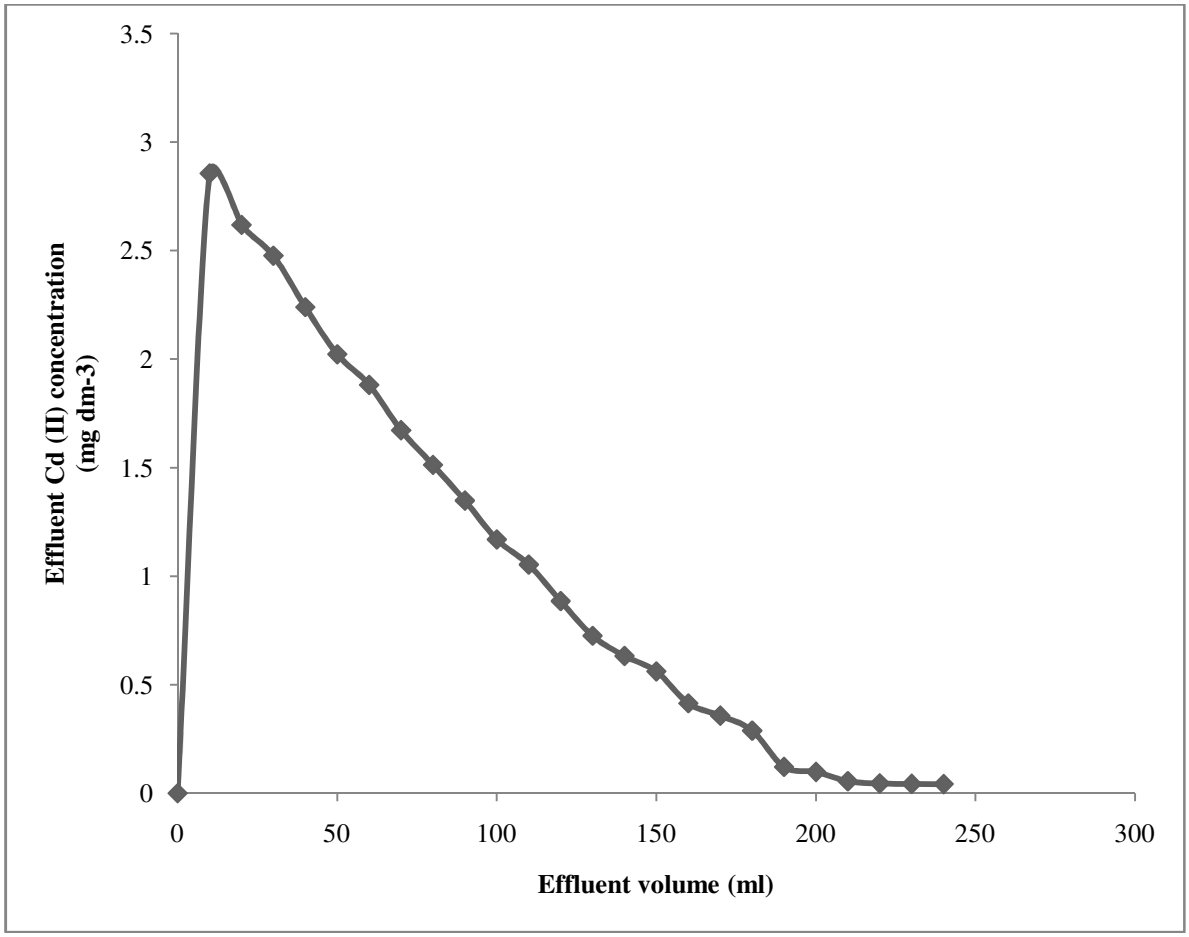

Figure-10
Desorption studies of Cd (II) ions using 0.1 M HNO_3 solution with Cd (II) adsorbed fix-bed micro column of nano iron oxide loaded PANA hydrogel at temperature = 25 ± 0.2°C, flow rate = 1 ml min^{-1} and bed depth = 1cm

References

1. Hutton M. and Symon C., Quantities of cadmium, lead, mercury and arsenic entering the environment from human activities, *Sci. Total Environ.,* **57,** 129-150 **(1986)**

2. Jin-ming LUO., Xiao XIAO. And Sheng-lian LUO., Biosorption of cadmium (II) from aqueous solutions by industrial fungus *Rhizopus cohnii*, *Trans. Nonferrous Met. Soc. China,* **20,** 1104-1111 **(2010)**

3. Low K.S. and Lee C.K., Cadmium uptake by the Moss, *Calymperes delessertii*, Besch, *Bioresource Technol.,* **38(1),** 1-6 **(1991)**

4. Salim R. Al-Subu M.M. and Sahrhage E., uptake of cadmium from water by beech leaves, *J. Environ. Sci. Health A,* **27,** 603-627 **(1992)**

5. Xiao X., Luo S., Zeng G., Wei W., Wan Y., Chen L., Guo H., Cao Z., Yang L., Chen J. and Xi Q., Biosorption of cadmium by Endophytic Fungus (EF) Microsphaeropsis sp. LSE 10 isolated from cadmium hyperaccumulator *Solanum Nigrum* L., *Bioresource Technol.,* **101(6),** 1668-1674 **(2010)**

6. Drash G.A., Increase of cadmium body burden for this century, *Sci. Total Environ.,* **67,** 75-89 (1993)

7. IARC, International Agency for Research on Cancer, *Monographs on the Evaluation of Carcinogenic Risks of Compounds,* IARC, New York, USA, **2,** p. 3974 **(1976)**

8. Sheng-lian LUO., Lin YUAN., Li-yuan CHAI., Xiao-bo MIN., Yun-yan WANG., Yan FANG. And Pu WANG., Biosorption behaviors of Cu^{2+}, Zn^{2+}, Cd^{2+} and mixture by waste activated sludge, *Trans. Nonferrous Met. Soc. China,* **16(6),** 1431-1435 **(2006)**

9. Yan H.E. and Gong-ming ZHOU., Research progress on excess sludge reduction technologies, *Environ.Technol.,* **1,** 39-42 **(2004)**

10. Hui LIU., Li-yuan CHAZ., Xiao-bo MIN., Yun-yan WANG. and Xia YU., Study and development of activated sludge treatment of heavy metal containing wastewater, *Ind. Water Waste.,* **35(4),** 9-11 **(2004)**

11. Tarley C.R.T. and Arruda M.A.Z., Biosorption of heavy metals using rice milling by-products: Characterization and application for removal of metals from aqueous effluents, *Chemosphere,* **54(7)**, 987-995 **(2004)**

12. Gupta A.K. and Wells S., Surface-modified superparamagnetic nanoparticles for drug delivery: preparation, characterization and cytotoxicity studies, *IEEE Transactions on Nanobioscience*, **3,** 66-69 **(2004)**

13. Ghorai S. and Pant K.K., Equilibrium, kinetics and breakthrough studies for adsorption of fluoride on activated alumina, *Sep. Purif. Technol.,* **42,** 265-271 **(2005)**

14. Sarin V., Singh T.S. and Pant K.K., Thermodynamic and breakthrough column studies for the selective sorption of chromium from industrial effluent on activated eucalyptus bark, *Bioresour. Technol.,* **97,** 1986-1993 **(2006)**

15. Taty-Costodes V.C., Fauduet H., Porte C. and Ho Y.S., Removal of lead (II) ions from synthetic and real effluents using immobilized Pinus sylvestris sawdust adsorption on a fixed-bed column, *J. Hazard. Mater.,* **123,** 135-144 **(2005)**

16. Vijavaraghavan K., Jegan J., Palanivelu K. and Velan M., Batch and column removal of copper from aqueous solution using brown marine alga *Turbinaria ornala*, *Chem. Eng. J.,* **106,** 177-184 **(2005)**

17. Ko D.C.K., Porter J.F. and Mckay G., Optimized correlations for the fixed-bed adsorption of metal ions on bone char, *Chem. Eng. Sci.,* **5,** 5819-5829 **(2000)**

18. Baral S.S., Das N., Ramulu T.S., Sahoo S.K., Das S.N. and Chaudhury G.R., Removal of Cr (VI) by thermally activated weed Salvinia cucullata in a fixed bed column, *J. Hazard. Mater.,* **161,** 1427-1435 **(2009)**

19. Chowdhury Z.Z., Zain S.M., Khan R.A., Rafique R.F. and Khalid K., Batch and fixed bed adsorption studies of lead (II) cations from aqueous solutions onto granular activated carbon derived from *Mangostana Garcinia* shell, *Bioresour.,* **7(3),** 2895-2915 **(2012)**

20. Ahmad A.A.and Hameed B.H., Fixed-bed adsorption of reactive azo dye onto granular activated carbon prepared from waste, *J. Hazard. Mater.,* **175,** 298-303 **(2010)**

21. Bohart G.S. and Adams E.Q., Some aspects of the behavior of charcoal with respect to chlorine, *J. Am. Che. Soc.,* **42(3),** 523-544 **(1920)**